Journal of Statistical Mechanics: Theory and Experiment
An IOP and SISSA journal

Imaging the stick–slip peeling of an adhesive tape under a constant load

Pierre-Philippe Cortet[1], **Matteo Ciccotti**[2] **and Loïc Vanel**[1]

[1] Laboratoire de Physique, CNRS UMR 5672, Ecole Normale Supérieure de Lyon, 46 allée d'Italie, 69364 Lyon Cedex 07, France
[2] Laboratoire des Colloïdes, Verres et Nanomatériaux, CNRS UMR 5587, Université de Montpellier II, Place Bataillon, 34095 Montpellier Cedex 5, France
E-mail: Loic.Vanel@ens-lyon.fr

Received 22 December 2006
Accepted 9 February 2007
Published 5 March 2007

Online at stacks.iop.org/JSTAT/2007/P03005
doi:10.1088/1742-5468/2007/03/P03005

Abstract. Using a high speed camera, we study the peeling dynamics of an adhesive tape under a constant load with a special focus on the so-called stick–slip regime of the peeling. It is the first time that the very fast motion of the peeling point has been imaged. The speed of the camera, up to 16 000 fps, allows us to observe and quantify the details of the peeling point motion during the stick and slip phases: stick and slip velocities, durations and amplitudes. First, in contrast with previous observations, the stick–slip regime appears to be only transient in the force controlled peeling. Additionally, we discover that the stick and slip phases have similar durations and that at high mean peeling velocity, the slip phase actually lasts longer than the stick phase. Depending on the mean peeling velocity, we also observe that the velocity change between stick and slip phases ranges from a rather sudden to a smooth transition. These new observations can help to discriminate between the various assumptions used in theoretical models for describing the complex peeling of an adhesive tape. The present imaging technique opens the door to an extensive study of the velocity controlled stick–slip peeling of an adhesive tape that will allow us to understand the statistical complexity of the stick–slip in a stationary case.

Keywords: dynamical processes (experiment), fracture (experiment), viscoelasticity (experiment), polymer dynamics

©2007 IOP Publishing Ltd and SISSA

Contents

1. Introduction

The peeling dynamics of adhesive tapes and especially its stick–slip complex regime has been at the centre of extensive investigations in recent years. The interest in such a phenomenon has two main justifications. Industrial processing often requires peeling ribbons of different kinds at very high velocities. In this situation, the stick–slip phenomenon and its jerky dynamics can cause important problems including delays on the assembly line. Additionally, understanding the physics of the adhesive tape peeling is valuable for modelling and testing the resistance of elastomer–substrate joints, and this seemingly simple system allows us to gain deeper insights into more subtle aspects of the physics of adhesion [1]. Despite extensive experimental and modelling efforts, our

J. Stat. Mech. (2007) P03005

understanding of the jerky behaviour experienced in the so-called stick–slip regime is still limited. The phenomenon remains highly non-linear and the dynamics shows a variety of instabilities and structures [2]. Several dynamical models have been developed with an increasing degree of realism, leading to an increasing complex dynamics [3]–[7]. Each model is characterized by a series of seemingly trivial assumptions which were progressively revealed to have a crucial effect on the dynamical aspects of the problem.

Due to the very rapid nature of the stick–slip dynamics, the main physical quantity generally accessed in the experiments is the distribution of the time intervals between successive events that can be identified through the measurement of the related acoustic or photonic emissions [2, 8]. In such experiments, an increasing irregularity of the stick–slip dynamics has been observed for an increasing peeling velocity. This behaviour is revealed to be more rich and complicated than a simple bifurcation route to chaos. In particular, one can observe hierarchical structures in a definite traction velocity range that can suggest the emergence of complexity.

Even though a lot of experimental studies of adhesive tape peeling have been performed, direct observation of the local motion of the peeling point in the stick–slip regime has not been done for the moment. In this paper, we present an experimental procedure for imaging directly, using a high speed camera, the dynamics at the peeling point, especially during the stick–slip phase (cf video 1). We test this technique in experiments where a constant load is applied to the tape. These very first experiments showing the true stick–slip dynamics of the peeling point in an adhesive tape already give very precise information that will help to screen among the various assumptions usually made in theoretical models. The technique opens the way to many more experimental investigations that should clarify the physics in operation in the peeling of an adhesive tape.

2. Previous experiments on adhesive tape peeling

The experiments on the peeling of an adhesive tape are generally performed using two different set-ups. In the first one, the peeling is studied when a constant traction velocity V is imposed onto the free end of the tape by the action of an electric motor. In this case, with a fixed geometry, V is the only dynamical control parameter. In a second type of experiment the peeling is studied when a constant applied load is clamped to the tape free end and the control parameter is the imposed force F. In these experiments, the limit between the adhesive tape ribbon and the free tape may be seen as a crack tip propagating at a speed v.

It is widely acknowledged in the literature [2]–[8] that there is a fundamental relation between the local peeling force f and the peeling velocity v at the peeling point (f is equal to the tensile force F at the free tape end in an idealized case where the peeling angle is 90° and the peeling is regular). A schematic representation of such a relation is plotted in figure 1. The sigmoidal shape of this curve, which is a consequence of the adhesive material rheology, presents three remarkable regions: two stable ones (I and III) and an unstable one (II). A full theoretical understanding of the shape of this curve is not available for the moment, but it has been acknowledged, at least since Prandtl [9], that such a dependence will lead to a hysteretic behaviour of the peeling point dynamics. A similar hysteresis of the force–velocity response is proposed to explain the pinning and

J. Stat. Mech. (2007) P03005

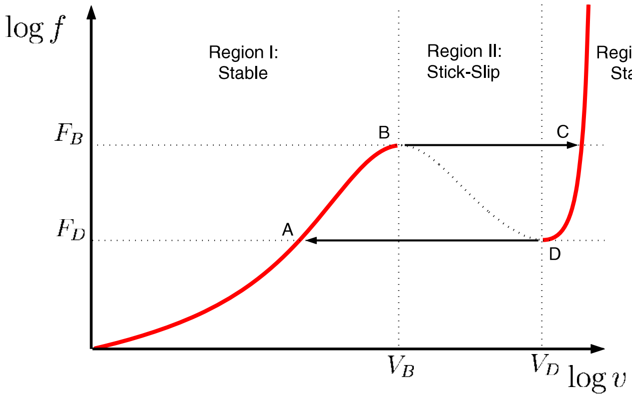

Figure 1. Schematic relation between the peeling force f and the peeling velocity v at the peeling crack line. These variables refer to the local dynamics of the peeling point and correspond to the tensile force F and velocity V at the free end of the tape only when the peeling is regular and the peeling angle is 90°. The sigmoidal shape is responsible for the hysteretic behaviour and therefore for the stick–slip dynamics.

depinning dynamics of charge-density waves, vortex arrays in semiconductors [10, 11] and possibly the stick–slip behaviour of contact lines [12] or magnetic domain walls [13].

Barquins and Maugis [14, 15] performed a series of experiments at constant traction velocity V. The observed dynamics exhibits the following behaviour: at slow traction velocity, the tape is peeled regularly and the dynamics is stationary (branch I); at high traction velocity, the dynamics is also regular, but much more rapid (branch III); in the intermediate range of V, a stick–slip phenomenon appears, the peeling of the tape being jerky with emission of a characteristic noise. In this regime, for increasing values of the traction velocity (from V_B to V_D), the stick–slip motion is at first rather periodic, then it becomes more and more irregular. It has been argued that the irregular motion corresponds to chaotic orbits [3]. In this regime, the local dynamics at the peeling point is expected to follow a complex trajectory, still not experimentally resolved, around the hysteretic region of the f–v curve.

In contrast, when a constant force f is applied to the peeling point, a stable regime always exists for the peeling (cf figure 1). However, for an applied force between F_D and F_B, there are two stable solutions, one on branch I (AB) and the other on branch III (DC) (cf figure 1). In experiments where the peeling was produced by a constant applied force F, with the help of a set of different dead loads clamped to the extremity of the free tape [8], several different regimes were observed for a given load depending on the way the experiment is started. The simplest experiment consists in applying the load instantaneously for an initial zero velocity of the peeling. In this case, where the initial condition of the peeling is out of equilibrium, the system reaches, for loads under F_B, a stable and regular peeling regime corresponding to branch I (branch A in figure 2). Forcing the peeling with a large enough initial velocity, it is possible to observe the stable and regular regime corresponding to branch III (branch C in figure 2) for loads over F_D. Moreover, an unexpected stick–slip regime was observed between the two stable branches (AB) and (DC), for loads between F_D and F_B, when introducing a moderate

doi:10.1088/1742-5468/2007/03/P03005

J. Stat. Mech. (2007) P03005

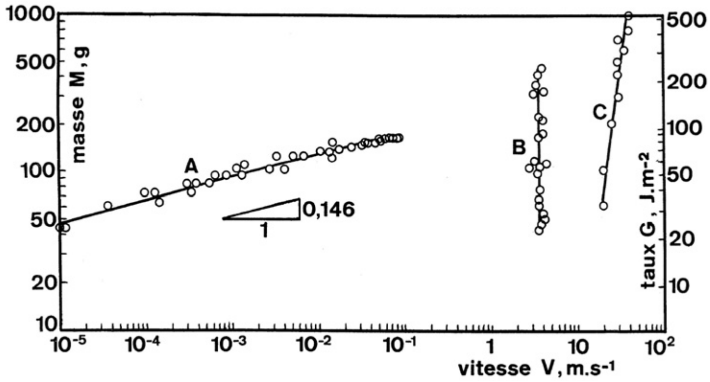

Figure 2. Applied mass as a function of the mean mass falling velocity $\langle v \rangle$ as reported in [8].

initial velocity to the peeling. The existence of this regime shows the metastability of the (AB) and (DC) branches and was attributed to the inertia of the falling load that cannot maintain instantaneously a constant force at the peeling point. In this regime, the local force and velocity at the peeling point are following cycles in the (ABCD) region of figure 1. Experimentally, it was observed that the time averaged value $\langle v \rangle$ of the peeling velocity in this stick–slip regime reaches a constant value that is almost insensitive to the load over one order of magnitude (cf figure 2). Finally, for loads over the critical load F_B (and typically less than $3F_B$) and an initial zero velocity of the peeling, a stick–slip regime arising spontaneously can be observed. The characteristics of this stick–slip regime are totally consistent with those observed for lower loads.

3. The experimental set-up

The results presented in this paper refer to experiments where an adhesive roller tape (3M Scotch® 600) is peeled off by applying a constant load. Actually, we attached a mass to the tape extremity and let it fall to the floor from a height of about 1.6 m with the roller mounted on a pulley rotating freely (cf figure 3). There is an additional pulley, between the roller and the mass, over which the non-adhesive side of the tape rolls. The distance between the pulley and the roller is 0.80 m. The adhesive tape and the basic loading scheme that have been used here are of the same kind as in [8]. In our experiment, we study the transient response of the peeling of the adhesive tape when a constant load is applied. More precisely, we introduce, depending on the load, different initial peeling velocities in order to enter the stick–slip regime during the fall.

The local dynamics of the peeling point has been imaged using a high speed camera (Photron Ultima 1024) at a rate of 8000 or 16 000 fps. The camera provides a 1024×1024 pixel^2 resolution when used at low frame rates. However, as the frame rate is increased, resolution is reduced. We get a very elongated image of 512×64 (resp. 256×32) pixel^2 at the frame rate of 8000 fps (resp. 16 000 fps). The elongated shape of the images leads us to focus on the peeling point region (cf figure 4). The longest direction of the image has been set perpendicular to the pulling direction of the applied load so as to maximize the resolution of the peeling point motion. One can see in figure 4 a typical

J. Stat. Mech. (2007) P03005

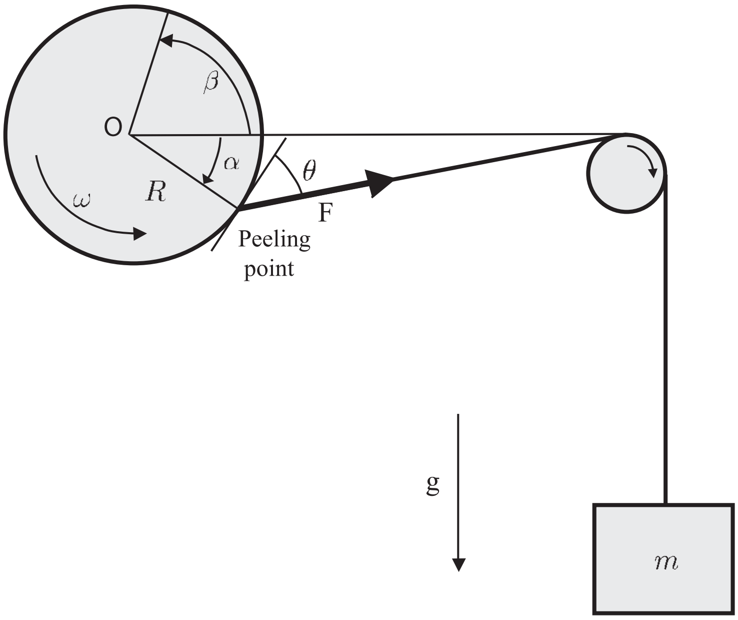

Figure 3. Experimental set-up and variables. The angles α and β are algebraic and oriented trigonometrically. Roller radius: 5.85 cm $> 2R >$ 3.65 cm, roller and tape width: 1.95 cm, tape thickness: 50 μm.

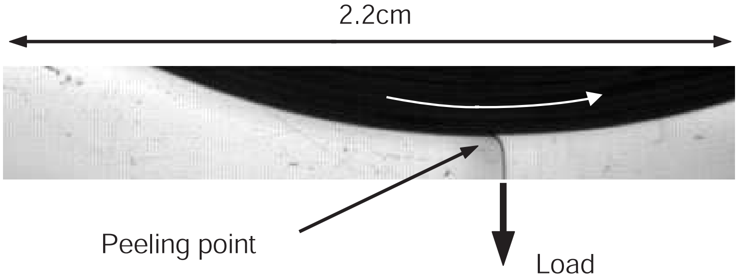

Figure 4. Image of the region near the peeling point (512×64 pixel^2).

image showing the peeling point, a part of the rotating roller and the beginning of the free tape. On the background, one can see defects of different sizes and shapes that actually are deposited on a transparent film that is attached to the tape roller. The rotational speed of these defects is therefore the same as the roller's.

The recording of each movie is synchronized with the arrival of the load on the ground level using a mechanical switch that generates a trigger signal when the falling load hits it. The camera works in a 'trigger end' mode, i.e. it keeps acquiring images until receiving the trigger signal. Consequently, in our movies, the last image corresponds to the moment when the load reaches the ground level.

4. The extraction of the peeling dynamics from the movies

The movies that have been recorded (cf video 1) allow us to access the curvilinear position of the peeling point $\ell_\alpha = R\alpha$ as well as the curvilinear position of the Scotch roller

J. Stat. Mech. (2007) P03005

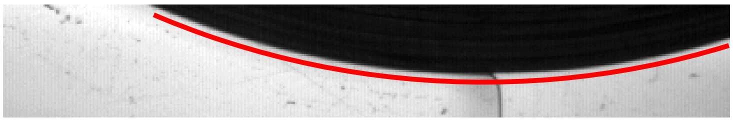

Figure 5. Image of the region near the peeling point (the same one as in figure 4) and the extracted pixel line on the circular shape.

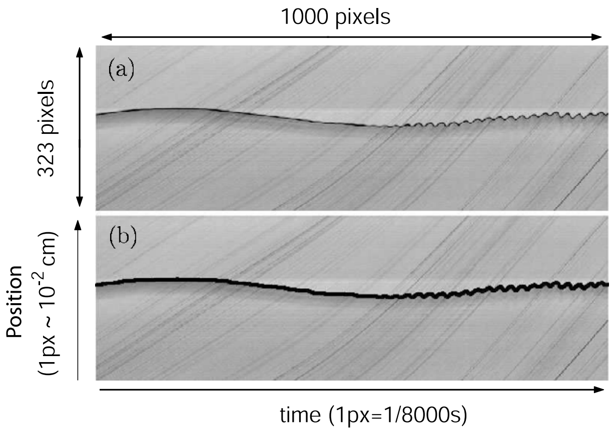

Figure 6. (a) Spatiotemporal image of the peeling point region. (b) Same image with superimposed the extracted position signal.

$\ell_\beta = R\beta$ in the laboratory reference frame as a function of time (α measures the angular position of the peeling point, β the rotation of the roller and R is the roller radius[3] (cf figure 3)). Once we know the position of the peeling point and the rotation of the roller in the laboratory reference frame, we can easily compute the curvilinear position of the peeling point $\ell_\gamma = \ell_\alpha - \ell_\beta$ in the roller reference frame and the corresponding angular position $\gamma = \alpha - \beta$.

In order to access ℓ_α and ℓ_β as a function of time, we extract for each image in a movie a line of pixels (solid line in figure 5) that follows the circular shape of the tape roller surface at a distance of a few pixels from this surface. This line of pixels is darker in a zone corresponding to the peeled ribbon. The pixel position of this zone gives with an analytical correction[4] the angular position of the peeled tape near the peeling point. Building an image with such an extracted pixel line for each time step of the movie leads to a spatiotemporal representation of the position of the peeling point as we can see in figure 6(a).

In such an image, we can extract the pixel position of the peeling point at each time step (cf figure 6(b)) and then have access to the full time-resolved curve of the peeling point position in the laboratory reference frame ℓ_α. We do this by correlating the typical grey-level profile around the peeling point with each pixels line. We have used the grey-level information in order to get subpixel accuracy on ℓ_α.

[3] R is obviously a function of time during a peeling experiment. Therefore, before each experiment, we measure the value of R. During one experiment, we neglect the variations of R that are less than 3%.

[4] The angular position ℓ_α is related to the pixel position n_{px} in the extracted pixels line as follows: $\ell_\alpha = R \arcsin((n_{\mathrm{px}} - n^0_{\mathrm{px}})/R)$ where n^0_{px} is the position of the roller axis.

J. Stat. Mech. (2007) P03005

The tilted dark lines, that one can see in the background of figure 6, correspond to the motion of the defects on the film that is attached to the roller. Their local slope represents the local rotational velocity of the roller. In order to have access to a full time-resolved motion of the roller, we actually built an image correlation technique that uses these defect lines. To improve the spatial resolution of the correlation technique, we have again used the grey-level information in order to get subpixel accuracy. In this manner, we are able to access the velocity $\dot{\ell}_\beta$ of the roller's rotation with an excellent precision. From the velocity signal, we can easily compute the roller position ℓ_β through numerical integration. A consistency check is performed by comparing the integrated position to the actual length of the peeled ribbon when the load reaches the ground.

5. Dependence of the peeling dynamics on the applied load and initial velocity

In our experiment, when applying a load to the tape extremity and starting from an initial zero peeling velocity, the peeling is regular and quickly reaches a stationary regime (cf video 2) for applied masses below a critical mass, $m_B = (235 \pm 5)$ g, with a slight dependence on the tape sample. The system quickly reaches equilibrium in the region I of figure 1 and the critical mass actually corresponds to the critical load F_B. In this regime, the mass falling velocity, that is equal to the average roller rotational velocity $\langle\dot{\ell}_\beta\rangle$, appears to be fairly constant during the fall and increases with the applied mass (for $m < m_B$) up to a value $v_c = (0.20 \pm 0.03)$ m s^{-1}. When m becomes larger than m_B, a stick–slip peeling dynamics appears spontaneously during the fall (cf video 1) along with a characteristic acoustic emission. Coincidentally, the mean velocity of the entire mass fall jumps to higher values. The initial condition in these experiments is out of equilibrium since it starts at the left end of the v-axis away from the f–v curve (cf figure 1). As has been noted in section 2, it is also possible to trigger a stick–slip dynamics for $m < m_B$ by introducing manually an initial velocity to the peeling.

In the following sections, we will present a detailed analysis of the transient peeling dynamics in the two cases where stick–slip has been heard of: $m < m_B$ with an initial velocity, $m > m_B$ without initial velocity. From now on, these two regimes will be referred to respectively as the triggered and spontaneous stick–slip regimes.

6. The rotation dynamics of the roller

6.1. Triggered case

In figure 7(a), we present the rotation velocity $\dot{\ell}_\beta$ of the roller as a function of time for a typical experiment performed with $m = 170$ g $< m_B$ in the case where the stick–slip has been triggered. First, we notice the initial acceleration of the rotation, with $\dot{\ell}_\beta$ getting from zero to about 1 m s^{-1}, that corresponds to the manual external forcing. Next, we see an oscillation of the rotation velocity at a frequency of about (9.8 ± 0.1) Hz and an amplitude of (0.50 ± 0.05) m s^{-1}. The amplitude of these oscillations is large. In figure 7(b), we present the corresponding acceleration of the roller $\ddot{\ell}_\beta$. In this figure, we see that the acceleration oscillates with time between (-11 ± 2) and (21 ± 2) m s^{-2}.

The acceleration oscillates around a non-zero average value (mean acceleration over an oscillation) of about 0.74 m s^{-2} over the whole fall of the mass. This leads to an increase

J. Stat. Mech. (2007) P03005

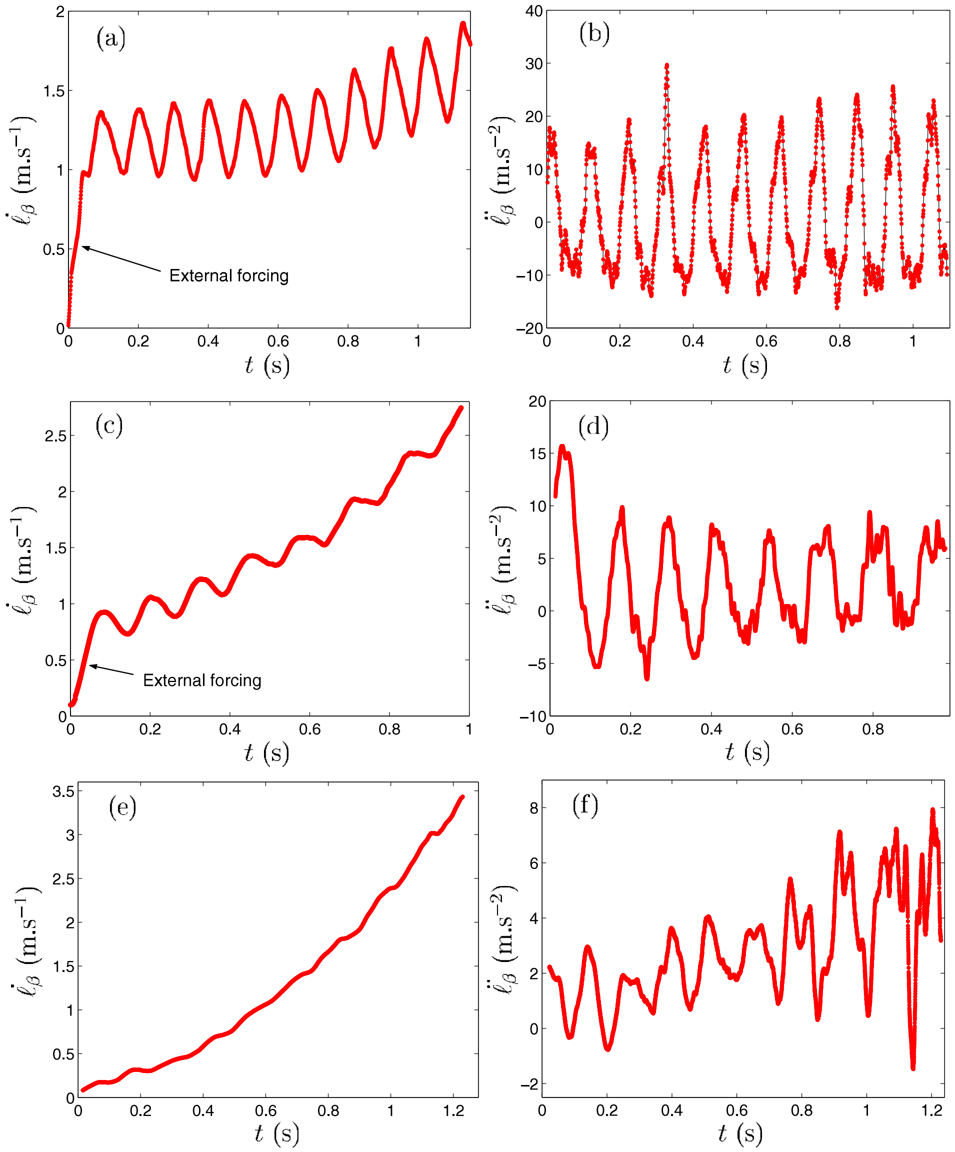

Figure 7. (a), (c) and (e), rotation velocity $\dot{\ell}_\beta$, (b), (d) and (f), corresponding (respectively to (a), (c) and (e)) acceleration $\ddot{\ell}_\beta$, as a function of the time. Curves (a)–(d) correspond to a triggered stick–slip peeling experiment performed with $m = 170$ g (curves (a) and (b)) and with $m = 195$ g (curves (c) and (d)). Curves (e) and (f) correspond to a spontaneous stick–slip peeling experiment performed with $m = 245$ g.

in the average rotation velocity from 1.15 to 1.65 m s^{-1}. This increase is related to an acceleration of the average peeling velocity $\langle v \rangle$ during the fall of the mass (cf section 7.2). We will see in the next section that the stick–slip heard during the fall of the mass has completely disappeared at the end of the fall and is therefore only a transient phenomenon.

As the applied mass is increased, we observe that the amplitude of the oscillations for the velocity and the acceleration decreases while the mean acceleration increases ($m = 195$ g $< m_B$ in figures 7(c) and (d)).

6.2. Spontaneous case

In figure 7(e), we present the rotation velocity $\dot{\ell}_\beta$ of the roller as a function of time for a typical experiment performed with $m = 245$ g $> m_B$ in the case where the stick–slip is spontaneous. Like in the triggered case, we see an oscillation of the rotation velocity at a frequency of about (8.5 ± 0.1) Hz. The amplitude of this oscillation is however much smaller than in the triggered case: (0.015 ± 0.005) m s^{-1}. In contrast, as one can see in figure 7(f), the mean acceleration over an oscillation of the rotation of the roller during the fall of the mass is larger and it gradually increases from 1 to 4 m s^{-2}. This non-zero mean acceleration results in an important increase in the mean velocity from zero to about 3.5 m s^{-1}. As for the triggered case, the stick–slip reveals to be only a transient phenomenon in these conditions (cf section 7.1).

We should point out that the observed increasing acceleration, in both the triggered and spontaneous cases, is inconsistent with the observation of an asymptotic constant velocity in the force controlled stick–slip regime as reported in [8].

6.3. The velocity oscillations

The origin of the velocity oscillations can be understood as a consequence of the interplay between the inertia of the roller and the moment applied to the roller by the peeling force. Since the oscillations exist even when there is no stick–slip, it is not necessary to take into account the stick–slip variations of the peeling force to explain the oscillations. However, it is important to take into account the acceleration a of the load which reduces the tensile force on the peeling point: $F = m(g - a)$.[5] Since the length of the peeled tape is long compared to the radius of the roller, we will assume that the direction of the tensile force is horizontal (i.e. $\theta \simeq \pi/2 + \alpha$). The basic equation of motion for the roller is then

$$I\ddot{\beta} = -m(g - a)R \sin\alpha \tag{1}$$

where I is the moment of inertia of the roller. In this equation, since it evolves quite slowly in time, we will consider a to be a constant parameter and estimate it using $a = \langle \ddot{\ell}_\gamma \rangle_T$, where T is the period of the velocity oscillation. Then, if we neglect the relative motion of the peeling point with respect to the roller (which is rather fast with respect to the velocity oscillations), we can write that $\gamma = \alpha - \beta = 0$. Thus, considering only small values of α, the roller's natural oscillation frequency is

$$\omega = \sqrt{\frac{m(g - \langle \ddot{\ell}_\gamma \rangle_T)R}{I}}. \tag{2}$$

In figure 8, we show the experimental oscillation frequency against the theoretical one $f_{\mathrm{th}} = \omega/2\pi$. We observe that there is a reasonable quantitative agreement between the two frequencies that confirms the relevance of equation (2) even though a lot of approximations have been used. Taking into account the motion of the peeling point would lead to corrections on the predicted frequency that are typically smaller than the experimental scatter of the data.

[5] It is almost rigorously true that $a = \ddot{\ell}_\gamma$.

J. Stat. Mech. (2007) P03005

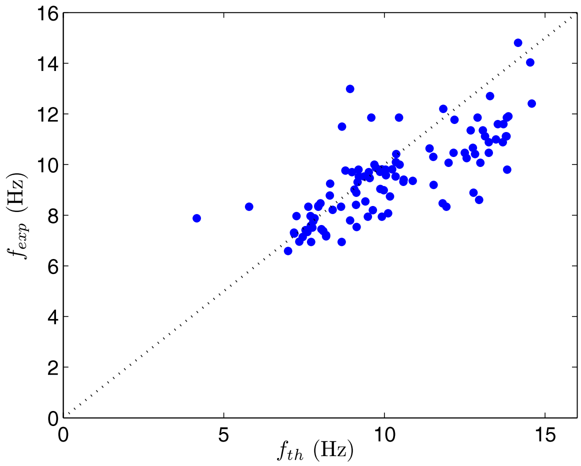

Figure 8. Experimental oscillation frequency as a function of the theoretical prediction (cf equation (2)), taking into account the accelerated motion of the load. The data correspond to different applied masses $m = 170, 195, 245, 265$ g, various radii 5.60 cm $> R >$ 3.60 cm and different moments during the fall of the mass.

7. The peeling point dynamics

7.1. In the laboratory reference frame

The main concern of this paper is to explore the rapid stick–slip dynamics of the peeling point and access directly variables that were previously only guessed through acoustic or photonic emissions. Consequently, we will in this section have a closer look at the peeling point motion during the stick–slip regime.

7.1.1. Triggered case. In figure 9, we present the full spatiotemporal image of the peeling point region, built according to the process exposed in section 4, for a typical triggered stick–slip experiment performed with $m = 195$ g $< m_B$.

This spatiotemporal image contains a lot of information. First, we note that there are low frequency oscillations of the peeling point position. There is a clear correlation between these oscillations and the one observed for the roller's rotation velocity. This correlation was expected since the moment on the roller resulting from the applied tensile force F depends on the angle α, and thus on the position of the peeling point in the laboratory reference frame. Next, during the early stage, we can note the huge curvature of the background black lines that corresponds to the initial acceleration due to external forcing. The stick–slip actually starts to develop during this phase. Then, its amplitude grows with time. However, later during the experiment, the stick–slip amplitude decreases back until a complete disappearance of the stick–slip motion occurs. This evolution of the peeling dynamical features occurs while the mean peeling velocity is increasing. Whether this eventually leads the system to reach an equilibrium state corresponding to branch III of figure 1 or not is still unclear.

In figure 10, we show part of the stick–slip motion signal extracted from the spatiotemporal image. The stick (resp. slip) phase corresponds to an increase (resp. decrease)

J. Stat. Mech. (2007) P03005

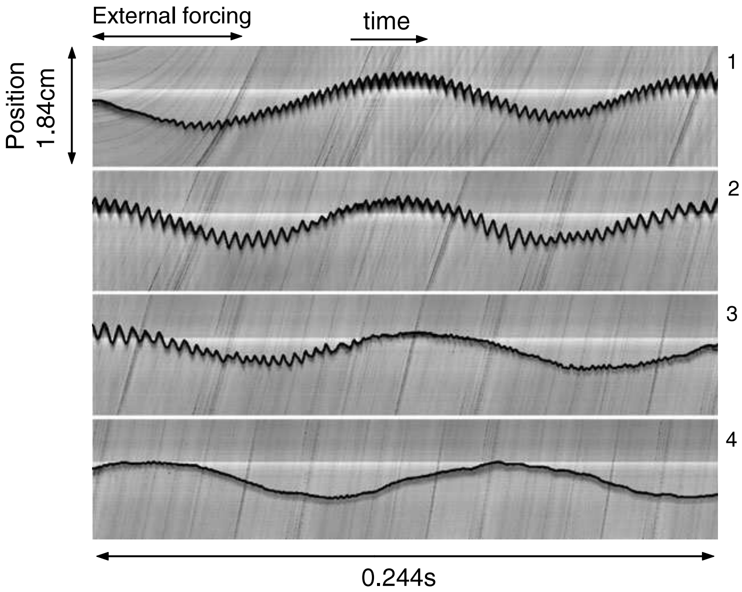

Figure 9. Spatiotemporal image of the peeling point region for a triggered stick–slip peeling experiment performed with $m = 195$ g. The extracted peeling point position has been added in black.

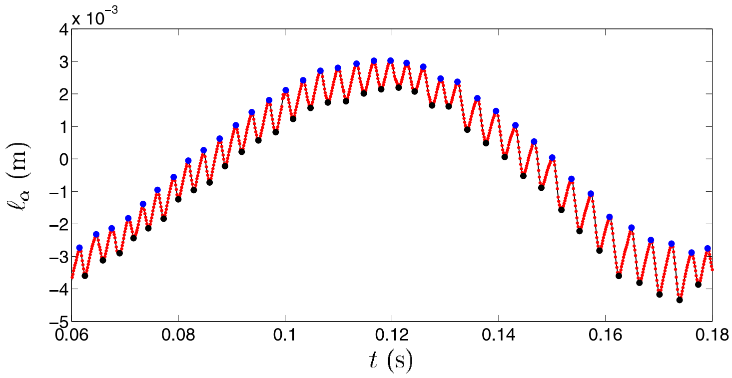

Figure 10. Position of the peeling point in the laboratory reference frame, ℓ_α, as a function of time for a triggered stick–slip peeling experiment performed with $m = 195$ g.

of ℓ_α. From such a signal, we have been able to study the evolution of the stick–slip amplitude, durations and velocities (stick and slip) as a function of time.

7.1.2. Spontaneous case. In figure 11, we present the full spatiotemporal image of the peeling point region for a typical spontaneous stick–slip experiment performed with $m = 245$ g $> m_B$.

As in the previous paragraph, there is a low frequency oscillation of the peeling point position, but with a smaller amplitude that corresponds to the decrease of the roller's oscillations amplitude with m that has been noted in the previous section. The stick–slip peeling is not initially present at the beginning of the experiment. It starts to

J. Stat. Mech. (2007) P03005

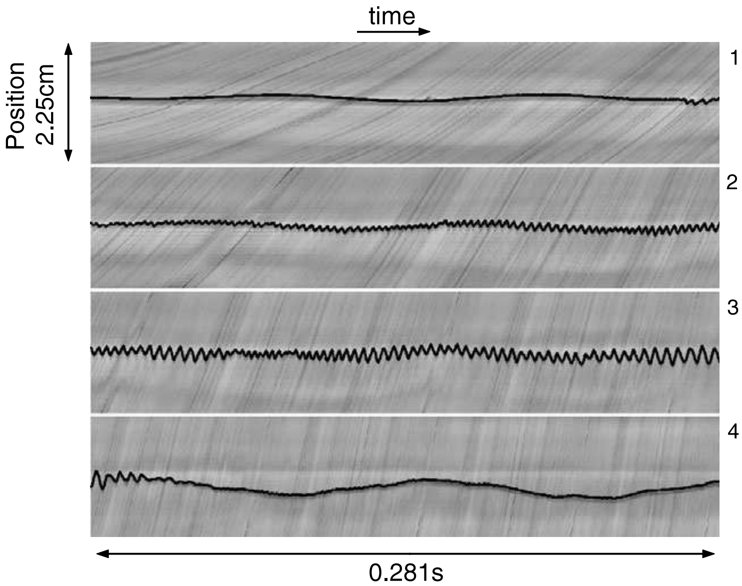

Figure 11. Spatiotemporal image of the peeling point region for a spontaneous stick–slip peeling experiment performed with $m = 245$ g. The extracted peeling point position has been added in black.

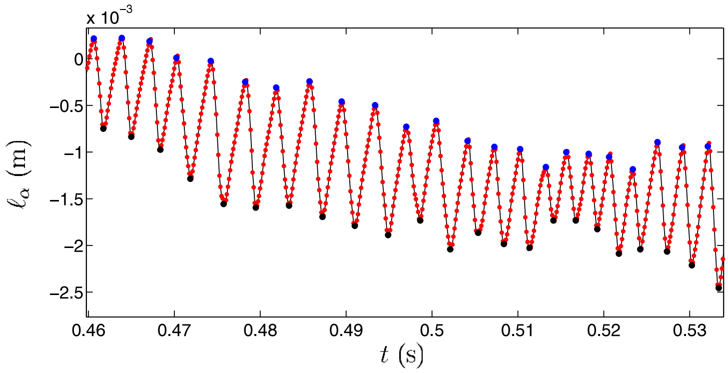

Figure 12. Position of the peeling point in the laboratory reference frame, ℓ_α, as a function of time for a spontaneous stick–slip peeling experiment performed with $m = 245$ g.

develop and grow after a certain time before its amplitude decreases back until a complete disappearance of the stick–slip motion occurs. Part of the extracted stick–slip signal is shown in figure 12.

To conclude this subsection, it is important to emphasize that the stick–slip regime of the force controlled peeling appears, in our experiments, to be only a transient phenomenon. This transient behaviour is clearly correlated with the increase in average peeling velocity that is observed during the fall of the mass. It is likely that the velocity will reach some elevated value on branch III of figure 1, but this evolution cannot be observed with the present set-up. This result is in contradiction with the existence of a stable stick–slip branch with a constant average velocity as suggested in [8]. This inconsistency is at

J. Stat. Mech. (2007) P03005

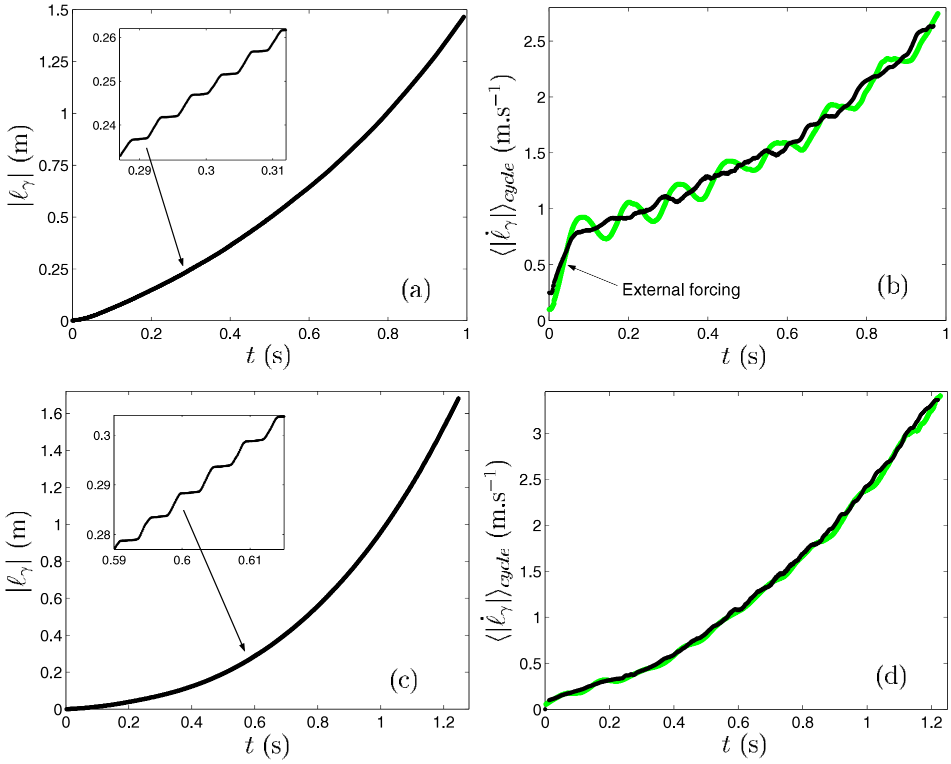

Figure 13. (a) and (c), absolute value of the peeling point position in the roller reference frame ℓ_γ as a function of time. The insets are zooms of these curves in a zone where stick–slip is observed. (b) and (d), corresponding (respectively to (a) and (c)) mean velocity of the peeling point (averaged over a stick–slip cycle) $\langle|\dot{\ell}_\gamma|\rangle_{\text{cycle}}$ as a function of time. The light grey (green) curves correspond to the velocity of the roller in the laboratory reference frame $\dot{\ell}_\beta$. Curves (a) and (b) correspond to a triggered stick–slip peeling experiment performed with $m = 195$ g. Curves (c) and (d) correspond to a spontaneous stick–slip peeling experiment performed with $m = 245$ g.

present not explained and could be due to a difference in moment of inertia of the roller. We can highlight that in [8] the presence of stick–slip in the experiments corresponding to branch B of figure 2 was only inferred from the presence of acoustic emissions. In contrast, the present experiment allows us to access directly the peeling point motion and to resolve the appearance and disappearance of stick–slip motion.

7.2. In the roller reference frame

In sections 6 and 7.1, we have extracted the peeling point position ℓ_α and the position of the roller ℓ_β in the laboratory reference frame. We are now able to determine the peeling point position in the roller reference frame $\ell_\gamma = \ell_\alpha - \ell_\beta$ which is the most relevant variable of the problem.

7.2.1. Triggered case. In figures 13(a) and (b), we show an example of the position and corresponding velocity of the peeling point in the roller reference frame in the triggered

J. Stat. Mech. (2007) P03005

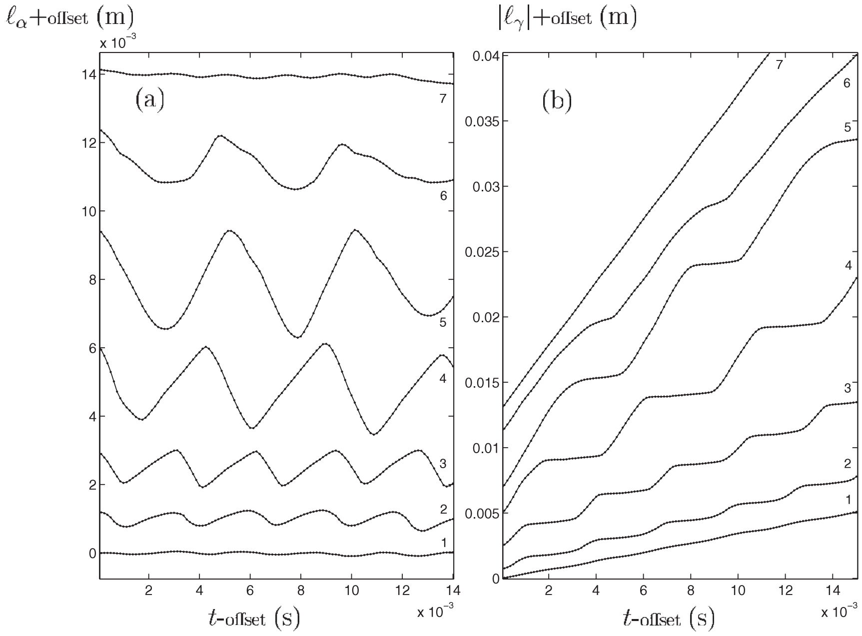

Figure 14. (a) Peeling point position in the laboratory reference frame at different moments (time is increasing with the item number) of a spontaneous stick–slip experiment performed at $m = 245$ g. (b) Same data in the roller reference frame.

case. We note that there is an abrupt increase in the initial velocity that is the result of the external forcing needed to trigger stick–slip. We also see that the low frequency oscillations observed on the rotation velocity of the roller have almost disappeared on the velocity of the peeling point in the roller reference frame (cf figure 13(b)).

7.2.2. Spontaneous case. In figures 13(c) and (d), we show the position and corresponding velocity of the peeling point in the roller reference frame in the spontaneous stick–slip case. In contrast with the triggered case, the initial velocity increases smoothly from zero. Similarly, the oscillations observed in the laboratory reference frame have almost disappeared in the roller reference frame.

7.3. Qualitative evolution of the peeling point dynamics

In figure 14, one can see the peeling point position in the laboratory reference frame, ℓ_α (cf figure 14(a)), and in the roller reference frame, $|\ell_\gamma|$ (cf figure 14(b)) at different moments of a spontaneous stick–slip experiment performed at $m = 245$ g. These figures show qualitatively the changes in the stick–slip characteristics during the experiment. The stick–slip amplitude and duration increase quite slowly with time (curves 1–5) before abruptly decreasing back (curves 5–7). We also see that the shape of the stick–slip cycle is changing. A more quantitative study of the evolution of the amplitude and duration as a function of the average peeling velocity is presented in section 8.

In figure 14(b), we see that the sharpness of the transition between the stick and slip phases evolves during the experiment as the peeling velocity increases. Actually, the transition is smooth when the stick–slip just starts to appear at low velocity or when it is

J. Stat. Mech. (2007) P03005

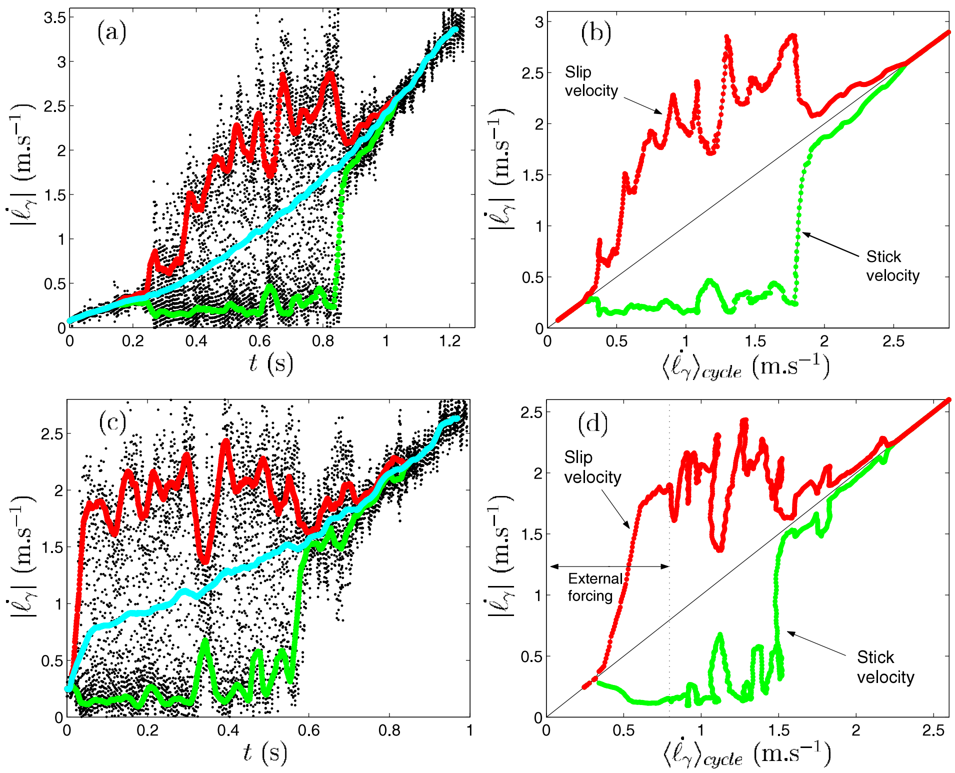

Figure 15. (a) and (c), instantaneous peeling velocity $|\dot{\ell}_\gamma|$ (black dots), average peeling velocity $\langle\dot{\ell}_\gamma\rangle_{cycle}$ (middle curve), average stick (bottom curve) and slip (top curve) velocities as a function of time. (b) and (d), corresponding (respectively to (a) and (c)) average stick and slip velocities as a function of the average peeling velocity. Curves (a) and (b) correspond to a spontaneous stick–slip peeling experiment performed with $m = 245$ g. Curves (c) and (d) correspond to a triggered stick–slip peeling experiment performed with $m = 195$ g.

close to disappearing at high velocity. In the intermediate velocity region, the stick–slip transition tends to be sharper. We also note that, when the stick–slip regime is close to disappearing, the slip to stick transition tends to become much smoother than the stick to slip transition.

8. The stick–slip average properties as a function of the mean peeling velocity

In this section, we present results that have been extracted from the two previously presented experiments performed with $m = 195$ and 245 g. However, the behaviour that will arise from these experiments is reproducible from one experiment to the other for the same experimental conditions.

8.1. Stick and slip velocities

8.1.1. Spontaneous case. From the position signal of the peeling point in the roller reference frame, we compute the instantaneous velocity and plot it as a function of time (black dots in figure 15(a)). The observed large velocity fluctuations are a signature of

J. Stat. Mech. (2007) P03005

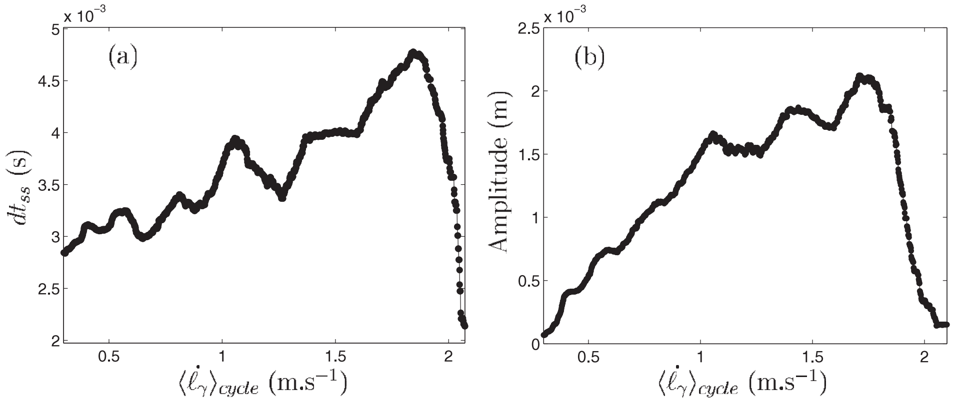

Figure 16. (a) Stick–slip cycle duration and (b) amplitude (in the laboratory reference frame) as a function of the average peeling point velocity for a stick–slip peeling experiment performed with $m = 245$ g.

J. Stat. Mech. (2007) P03005

the stick–slip motion. We extract from this instantaneous velocity the mean stick and slip velocities averaged over a few stick–slip cycles (cf figures 15(a) and (b)). The stick–slip motion initiates at a peeling velocity of about 0.25 m s^{-1} with average stick and slip velocities starting to deviate from the average peeling velocity. This velocity corresponds well to the maximum velocity reachable in a stable peeling experiment (0.20 ± 0.03) m s^{-1}. When the average velocity increases further, the stick velocity remains quite stable with a value of 0.2–0.3 m s^{-1}. It is important to note that the average stick velocity remains close to the peeling velocity just before the transition towards stick–slip. In contrast, the slip velocity increases gradually from about 0.25 m s^{-1} up to 2.6 m s^{-1}. The fluctuations that are observed on the slip velocity, and to a lesser extent on the stick velocity, are correlated with the low frequency oscillation of the average peeling position. This shows that there is a dependence of the stick–slip properties on the angle α. The stick–slip reduces in amplitude for an average peeling velocity of 1.8 m s^{-1} and finally totally disappears for an average peeling velocity of 2.6 m s^{-1}.

In the triggered case, the external forcing brings the average peeling velocity to a value close to 0.8 m s^{-1}. The stick–slip motion is initiated during this loading phase. For average velocities larger than 0.8 m s^{-1}, both the stick and slip velocities remain rather stable, despite some fluctuations, until the stick–slip reduces its amplitude and finally disappears (cf figures 15(c) and (d)). By comparing figures 15(b) and (d) we can see a similar behaviour for similar values of the average peeling velocity.

8.2. Stick–slip periods and amplitudes

In figure 16, we show the period and amplitude of stick–slip as a function of the peeling velocity for a typical experiment in the spontaneous case. We observe that the period range is 2–5 ms and the amplitude range is 0–2 mm. Both the period and amplitude are increasing with the peeling velocity. When reaching a peeling velocity of about 1.8 m s^{-1}, the strong observed reduction in the stick–slip amplitude (down to zero) is associated with a reduction of the stick–slip period.

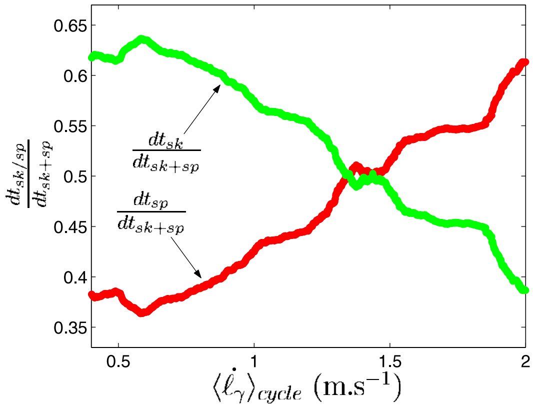

Figure 17. Ratio of the stick (light grey/green points) and slip (strong grey/red points) phases duration with the stick–slip duration as a function of the average peeling point velocity for a stick–slip peeling experiment performed with $m = 245$ g.

8.3. Relative stick and slip durations

Another important feature of the stick–slip motion is that the relative durations of the stick and slip phase are evolving with the average peeling velocity. In figure 17, we show the fraction of time during a stick–slip period spent in the stick and in the slip phase. Remarkably, there is never more than a factor of 2 between the stick duration and the slip duration. This observation rules out models where the slip duration was assumed to be much shorter than the stick one. Even more remarkably, the stick duration, initially about twice the slip duration, gradually decreases with the peeling velocity and becomes smaller than the slip duration, down to almost one half.

These results might look surprising compared to the usual frictional stick–slip phenomenon. Indeed, in the case of the traditional spring–block experiment stick–slip [16, 17], the stick phase is often expected to be much longer compared to the slip phase. However, the slip phase duration can become comparable to the stick phase one when the system is near to the threshold of stick–slip appearance [17, 18]. In contrast, for the stick–slip peeling of an adhesive tape, this remains true far from the threshold.

9. Discussion

In this paper, we have presented the results of a direct fast imaging of the stick–slip peeling of an adhesive tape under force controlled conditions. The motion of the roller and of the peeling point are measured in the laboratory reference frame with an excellent resolution in order to study at the same time the global dynamics of the system and the details of the peeling dynamics. In these experiments, whether the stick–slip is spontaneous or triggered, we observed that it is only a transient phenomenon that happens in conjunction with a progressive acceleration of the falling load. The velocity at which the stick–slip appears spontaneously is close to the limit velocity for the regular peeling (about 0.2 m s^{-1}). Then, for an increasing average peeling velocity, the stick–slip amplitude grows before it abruptly reduces at a velocity of about 1.8 m s^{-1}, and finally disappears completely at 2.6 m s^{-1}.

J. Stat. Mech. (2007) P03005

In all our observations, the peeling was shown to be accompanied by an oscillation in the roller velocity at about 10 Hz that can be modelled in terms of the harmonic torque induced by the oscillations of the peeling point angle. These oscillations have an influence on the characteristics of the stick–slip such as period and amplitude. The duration of the stick and slip phases is revealed to be comparable (ratio from 0.5 to 2), with a longer stick duration at low peeling velocity and a longer slip duration at large peeling velocity. The sharpness of the transition between the stick and slip phases evolves during an experiment as the mean peeling velocity increases. Actually, the transition is smoother when the stick–slip just starts to appear at low velocity or when it is close to disappearing at high velocity. In the intermediate range of velocity, the stick–slip transition tends to be sharper.

Our data are in contradiction with the existence of a stable stick–slip branch with constant average velocity as suggested in [8]. We can highlight that in [8] the presence of stick–slip in the experiments for the branch B of figure 2 was only inferred from the presence of acoustic emissions during the test. To overcome this contradiction, we plan to acquire acoustic emissions in parallel to the imaging of the peeling point motion. It is also important to check whether increasing the falling height of the mass in our experiment would help in reaching a stationary peeling regime or not.

The measurement technique that we have developed is precise enough to make quantitative comparison with theoretical models. In order to clarify the physics in operation in the peeling of an adhesive tape, more experimental work will be necessary. For instance, understanding the complex stick–slip statistics at high peeling rate [2] will require studies in the velocity controlled regime for which the stick–slip dynamics is stationary.

Acknowledgment

We thank S Ciliberto for insightful discussions.

References

[1] Ryschenkow G and Arribart H, 1996 *J. Adhes.* **58** 143
[2] Ciccotti M, Giorgini B, Vallet D and Barquins M, 2004 *Int. J. Adh. Adh.* **24** 143
[3] Hong D C and Yue S, 1995 *Phys. Rev. Lett.* **74** 254
[4] Ciccotti M, Giorgini B and Barquins M, 1998 *Int. J. Adh. Adh.* **18** 35
[5] De R, Maybhate A and Ananthakrishna G, 2004 *Phys. Rev.* E **70** 046223
[6] De R and Ananthakrishna G, 2005 *Phys. Rev.* E **71** 055201
[7] De R and Ananthakrishna G, 2006 *Phys. Rev. Lett.* **97** 165503
[8] Barquins M and Ciccotti M, 1997 *Int. J. Adh. Adh.* **17** 65
[9] Prandtl L, 1928 *J. Appl. Math. Mech.* **8** 85
[10] Vinokur V M and Nattermann T, 1997 *Phys. Rev. Lett.* **79** 3471
[11] Marchetti M C, Middleton A A and Prellberg T, 2000 *Phys. Rev. Lett.* **85** 1104
[12] Schäffer E and Wong P Z, 2000 *Phys. Rev.* E **61** 5257
[13] Urbach J S, Madison R C and Markert J T, 1995 *Phys. Rev. Lett.* **75** 4694
[14] Barquins M, Khandani B and Maugis D, 1986 *C. R. Acad Sci. Paris* **303** 1517
[15] Maugis D and Barquins M, 1988 *Adhesion* 12th edn, ed K W Allen (London: Elsevier Applied Science) p 205
[16] Johansen A, Dimon P and Ellegaard C, 1994 *Wear* **172** 93
[17] Baumberger T and Caroli C, 2006 *Adv. Phys.* **55** 279
[18] Heslot F, Baumberger T, Perrin B, Caroli B and Caroli C, 1994 *Phys. Rev.* E **49** 4973